Strain determination in PbEuTe/PbTe multi-quantum wells

E. Abramof,[a] P. H. O. Rappl, A. Y. Ueta, and P. Motisuke
Instituto Nacional de Pesquisas Espaciais - INPE, Laboratório Associado de Sensores e Materiais - LAS, CP 515, 12201-970 São José dos Campos-SP, Brazil

(Received 14 January 2000; accepted for publication 17 April 2000)

A series of $Pb_{1-x}Eu_xTe$/PbTe multi-quantum well (MQW) samples were grown on (111) cleaved BaF_2 substrates by molecular beam epitaxy. The Eu content was maintained at $x \sim 0.05-0.06$ and the PbTe well width was varied from 23 to 206 Å. The samples were characterized structurally by high resolution x-ray diffraction in the triple axis configuration. The $\omega/2\Theta$ scans of the (222) Bragg reflection showed very well resolved satellite peaks up to the tenth-order for all samples indicating that sharp interfaces were obtained. Reciprocal space mapping around the (224) lattice point indicated that the MQW structure tended to the free-standing condition. The (222) $\omega/2\Theta$ scans were calculated by dynamical theory of x-ray diffraction and compared to the measured ones. Using the in-plane lattice constant as the main fitting parameter, the strain in the PbTe well inside the MQW structure was obtained as a function of its width. It decreased monotonically from an almost fully strained layer to 26% of strain relaxation as the PbTe well increased from 23 to 206 Å. © *2000 American Institute of Physics.* [S0021-8979(00)06414-8]

I. INTRODUCTION

PbTe and EuTe crystallize in the rocksalt structure and the lattice mismatch between these materials is relatively small (~2%). The energy gap of EuTe (2 eV) is much higher than that of PbTe (310 meV at 295 K). In this sense, only a small Eu content in the ternary $Pb_{1-x}Eu_xTe$ is sufficient to produce large barriers in the PbEuTe/PbTe heterostructure. For instance, $Pb_{1-x}Eu_xTe$ with $x=0.06$ ($Eg=530$ meV at 295 K) yields a barrier of 110 meV in the $Pb_{1-x}Eu_xTe$/PbTe heterostructure, considering a band offset of 50%.[1] These material properties make the PbTe–EuTe system suitable for the fabrication of multi-quantum well structures.

Molecular beam epitaxy (MBE) has been successfully applied for the growth of $Pb_{1-x}Eu_xTe$ layers and respective PbEuTe/PbTe multi-quantum wells (MQWs).[2,3] The measurement of quantum Hall effect in these heterostructures has attested to the high quality of the grown layers and interfaces.[4] Infrared transmission measurements have been performed to determine the optical transition energies between the confined states in the PbEuTe/PbTe MQW samples.[5,6] The electronic states and respective optical transitions of lead salt QWs have been calculated and reasonable agreements with the experiments have been obtained.[7,8]

PbEuTe/PbTe MQWs find their main application in diode lasers emitting in the mid-infrared range.[9,10] As the quantized levels depend strongly on the strain inside the MQW, it is important to have reliable methods to determine the strain in these structures. High-resolution x-ray diffraction has been applied in the structural characterization of PbTe-based multilayer systems,[11,12] but no systematic study has been reported so far. This work is dedicated to the determination of strain inside PbEuTe/PbTe MQW structures as a function of the PbTe well width, using high-resolution x-ray diffraction analysis.

A series of $Pb_{1-x}Eu_xTe$/PbTe MQW samples was grown by molecular beam epitaxy where the Eu content is maintained at $x \sim 0.05-0.06$ and the PbTe well width is varied in the range of 20–200 Å. Detailed structural characterization was made by high-resolution x-ray diffraction using the triple axis configuration. The $\omega/2\theta$ scans of the (222) Bragg diffraction peak were measured for all samples. The MQW period, the thickness of individual barrier and well layers, and the buffer lattice constants were obtained. In order to give a better insight into the strain state inside the MQW, reciprocal space maps were measured around the asymmetrical (224) lattice point. From the information obtained from these maps, the (222) $\omega/2\theta$ spectra were calculated by dynamical theory of x-ray diffraction using Takagi–Taupin equations and compared to the measured ones. From this fitting process, the strain in the MQW structure was determined for samples with different PbTe well widths.

II. SAMPLE GROWTH

The $Pb_{1-x}Eu_xTe$/PbTe MQW samples were grown on freshly cleaved (111)BaF_2 by molecular beam epitaxy in a RIBER 32P MBE system equipped with PbTe, Eu and Te effusion cells.[13] A 12 keV reflection high-energy electron diffraction (RHEED) system was used to evaluate *in situ* the growth conditions.

Before properly growing the MQW structure, the growth of $Pb_{1-x}Eu_xTe$ single layers with low Eu content was carefully investigated. The BaF_2 substrates were preheated at 500 °C for 10 min before starting the growth. The deposition rate of PbTe, Eu and Te was monitored with a quartz crystal oscillator. The beam-flux rate ratio ($J_{Eu}/J_{PbTe}+J_{Eu}$) was used to estimate the nominal Eu concentration. For optimal growth conditions, the Te beam-flux rate was chosen to be

[a]Author to whom correspondence should be addressed; electronic mail: abramof@las.inpe.br

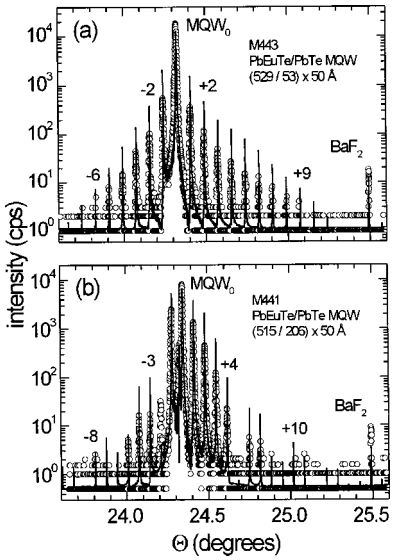

FIG. 1. The $\omega/2\theta$ scans of the (222) Bragg diffraction peak for two different PbEuTe/PbTe MQW samples with PbTe well width of (a) 53 Å (M443) and (b) 206 Å (M441). The open circle (○) represents the experimental data and the solid lines are the calculated spectra, which best fit to the measured data.

two times the one of Eu.[3] Just like PbTe, the growth of PbEuTe with low Eu content starts with a three-dimensional nucleation, evidenced by the spotty RHEED pattern. After 0.5–1 min (600–1200 Å), the initial islands coalesce and the RHEED pattern changes to a streaky one. When the layer thickness achieves approximately 0.5 μm, the RHEED pattern already shows elongated spots lying on a semicircle characteristic of an atomically flat surface. This RHEED pattern persists until the end of growth. No surface reconstruction is observed during the PbEuTe growth.

For the growth of the MQW samples, a $Pb_{1-x}Eu_xTe$ buffer layer (with the same x value as the barrier) was grown on top of the BaF_2 substrate. The buffer layer was approximately 4 μm thick in order to guarantee that it is completely relaxed and free from the defects originated from the three-dimensional nucleation at the initial growth stage. The growth temperature for the buffer and MQW structure was 300 °C. The PbTe and Te effusion cell shutter was always open during growth. The opening and closing times of the Eu shutter were chosen to obtain the desired thickness of the barrier and well, respectively. The number of repetitions of all MQW samples was chosen to be 50.

Two series of $Pb_{1-x}Eu_xTe$/PbTe MQW samples were produced. In these series the PbEuTe barrier is kept thicker than 440 Å and the PbTe well width is varied. The only difference between the two series was the growth rate, which is mainly determined by the PbTe effusion cell temperature (2.2 Å/s for the first series and 3.8 Å/s for the second). All other growth parameters were kept constant in order to guarantee sample reproducibility.

III. STRUCTURAL CHARACTERIZATION

The PbEuTe/PbTe MQW samples were characterized structurally by high-resolution x-ray diffraction analysis using Cu $K\alpha_1$ radiation. The x-ray diffraction measurements were carried out in a Philips X'Pert diffractometer in the triple axis configuration, which employs a four-crystal Ge(220) monochromator in the primary optics (between the Cu x-ray tube and the sample) and a Ge(220) channel-cut analyzer immediately before the detector (secondary optics). In this configuration, the incident x-ray beam has an axial divergence of 12 arcsec and a wavelength dispersion of approximately 2×10^{-4}. The acceptance angle of the detector is also reduced to 12 arcsec, increasing substantially the resolution in the 2θ direction.

The $\omega/2\theta$ scan of the (222) Bragg diffraction peak was measured for all samples. Figures 1(a) and 1(b) show the whole (222) $\omega/2\theta$ scan for two different MQW samples, namely M443 and M441, with PbTe well width of 53 and 206 Å, respectively. The general features of the measured $\omega/2\theta$ spectra can be summarized as follows. The zero-order peak (MQW_0) of the MQW structure appears as the most intense peak in all the spectra. The $\omega/2\theta$ spectra exhibit a very well resolved satellite peak structure showing up to the tenth-order. The intensity modulation of the satellite peak structure changes as the PbTe well width changes for the different MQW samples. The PbEuTe buffer layer peak appears on the lower angle side near the MQW_0 peak and for

TABLE I. Data of the $Pb_{1-x}Eu_xTe$/PbTe MQW samples obtained from the x-ray analysis: MQW period (P), barrier (d^{barrier}) and well (d^{well}) width, buffer lattice constant (a^{buffer}), Eu content (x), in-plane lattice constant ($a^{\text{in-plane}}$), free-standing lattice constant (a^{fs}), PbTe well parallel strain ($\epsilon_{||}^{\text{PbTe}}$), maximum possible parallel strain in PbTe well ($\epsilon_{||}^{\text{max}}$), and the fraction of maximum strain incorporated in PbTe well (PS).

Sample	P (Å)	d^{barrier} (Å)	d^{well} (Å)	a^{buffer} (Å)	x	$a^{\text{in-plane}}$ (Å)	a^{fs} (Å)	$\epsilon_{\|\|}^{\text{PbTe}}$ (10^{-3})	$\epsilon_{\|\|}^{\text{max}}$ (10^{-3})	$PS=(\epsilon_{\|\|}^{\text{PbTe}}/\epsilon_{\|\|}^{\text{max}})$
1st series										
M443	582	529	53	6.4808	0.060	6.479 33	6.4791	2.682	2.909	0.922
M440	622	518	104	6.4820	0.064	6.479 40	6.4787	2.693	3.095	0.870
M442	676	520	156	6.4808	0.060	6.477 65	6.4765	2.422	2.909	0.832
M441	721	515	206	6.4783	0.052	6.474 20	6.4736	1.888	2.522	0.748
2nd series										
M457	510	487	23	6.4775	0.049	6.477 00	6.4768	2.321	2.399	0.968
M462	502	457	45	6.4772	0.049	6.476 22	6.4758	2.201	2.352	0.936
M461	562	470	92	6.4763	0.046	6.473 97	6.4740	1.852	2.213	0.837
M460	600	460	140	6.4775	0.049	6.474 10	6.4739	1.872	2.399	0.781
M456	621	442	179	6.4784	0.052	6.475 0	6.4737	2.012	2.538	0.793

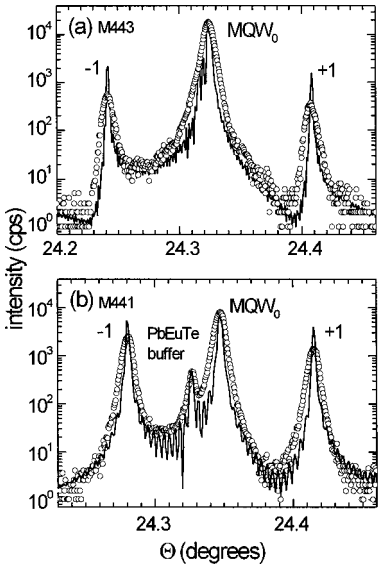

FIG. 2. Expanded scale near the zero-order satellite peak (MQW_0) of the (222) $\omega/2\theta$ scans plotted in Figs. 1(a) and 1(b), respectively.

samples with narrow PbTe well it is overlapped by the MQW_0. The BaF_2 substrate peak is observed with a small intensity, due to the absorption in the buffer layer plus MQW stack, and is used as a reference for the θ scale.

The MQW period was obtained from the angular separation between the satellite peaks. The individual thickness of the barrier and well was inferred from the Eu shutter opening and closing time, respectively. Since the Eu content was small ($\sim 0.05-0.06$), the growth rate in the MQW structure was mainly determined by the PbTe effusion cell temperature, leading to a maximum error of 5% in this individual thickness determination procedure. The values of the MQW period (P), PbEuTe barrier (d^{barrier}) and PbTe well (d^{well}) width obtained from the x-ray measurements are displayed in Table I for all MQW samples.

The PbEuTe buffer lattice constant (a^{buffer}) was determined using the BaF_2 substrate peak as a reference. The Eu content (x) of the $Pb_{1-x}Eu_xTe$ buffer layer was evaluated from a^{buffer} for each sample. The mean Eu content for the first series turned out to be 0.049 with a maximum variation of ± 0.003. For the second series, the mean Eu content was 0.059 with a maximum variation of ± 0.006. These data are also displayed in Table I.

The resolved satellite peak structure shown in Fig. 1 was observed for all samples. It indicates good thickness reproducibility from layer to layer, homogeneous Eu content through the MQW structure and very low interdiffusion in the interfaces, independent of the PbTe well width. The full width at half maximum (FWHM) of the MQW_0 peak was about 25 arcsec in the $\omega/2\theta$ direction and approximately three times larger in the ω direction.

Figures 2(a) and 2(b) plot the (222) $\omega/2\theta$ spectra of Figs. 1(a) and 1(b), respectively, in an expanded scale near the zero-order peak of the MQW structure including up to the two nearest satellite peaks. For the samples with narrow PbTe well [53 Å in case of Fig. 2(a)], the MQW zero order overlaps with the PbEuTe buffer layer peak, whereas, for

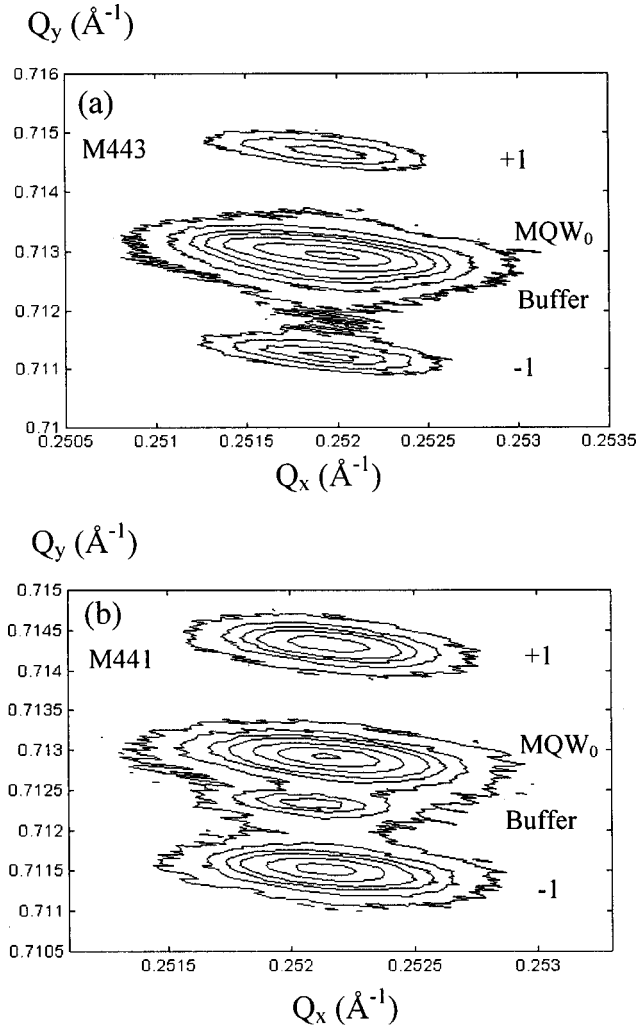

FIG. 3. Reciprocal space maps around the asymmetrical (224) lattice point for two PbEuTe/PbTe MQW samples. The maps are plotted in reciprocal coordinates Q_x parallel to the [11-2] in-plane azimuth and Q_y parallel to the [111] growth direction. The plotted region includes the buffer layer peak and the zero-order (MQW_0) plus two first-order (± 1) satellite peaks. (a) Sample M443 [(529/53)×50 Å] with isointensity contour lines at 10, 40, 120, 250, 600, 2000, and 5000 cps. (b) Sample M441 [(515/206)×50 Å] with isointensity contour lines at 10, 40, 100, 200, 600, 1500, and 3200 cps.

samples with wider PbTe well [206 Å in case of Fig. 2(b)], the PbEuTe buffer peak is well resolved and separated from the MQW_0. The position of the zero-order peak relative to the buffer layer peak contains important information about the strain inside the MQW samples.

IV. STRAIN DETERMINATION

Reciprocal space mapping around the (224) asymmetrical Bragg diffraction peak was performed in order to give a better insight into the strain state of the MQW structure. The reciprocal space maps are obtained by performing a set of $\omega/2\theta$ scans with different ω-offset angles. Figures 3(a) and 3(b) show the reciprocal space maps around the (224) reciprocal lattice point (RELP) for the samples M443 (PbTe well width of 53 Å) and M441 (PbTe well width of 206 Å), respectively. The maps include the MQW zero-order RELP (MQW_0), the buffer layer and the two first-order satellite

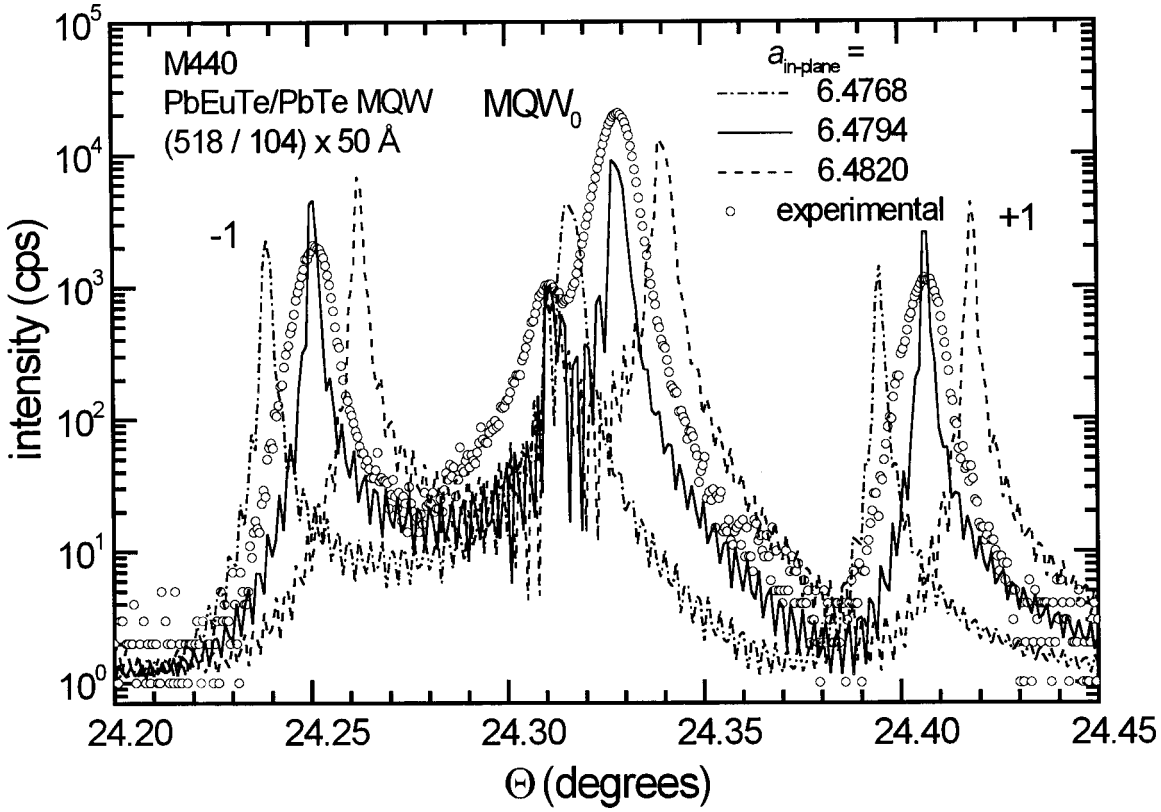

FIG. 4. The $\omega/2\theta$ scan near the zero-order (222) Bragg diffraction peak for the PbEuTe/PbTe MQW sample with PbTe well width of 104 Å (M440). The lines are the calculated spectra using different values of in-plane lattice constant ($a^{\text{in-plane}}$).

RELPs. They are plotted in reciprocal lattice coordinates Q_x parallel to the [11-2] in-plane azimuth direction (parallel to the sample surface) and Q_y parallel to the [111] growth direction. The ellipse-like curves in the maps are contour lines with equal intensity. The axis of the ellipses is inclined in relation to Q_x axis due to a broadening in ω direction caused by the mosaicity in the MQW samples.

In the map of Fig. 3(a) the buffer layer RELP is mixed with the MQW_0 RELP. Within the map resolution, the MQW structure has approximately the same horizontal coordinate Q_x as the buffer layer. However, in the map shown in Fig. 3(b) the buffer layer RELP appears well resolved separated from the MQW_0 RELP with its central position shifted in the Q_x axis with respect to the central positions of the MQW structure RELPs. These results indicate that the MQW structure does not remain pseudomorphic (same in-plane lattice constant) to the buffer layer. The MQW structure tends to the free-standing condition.

The in-plane lattice constant for the free-standing state can be calculated using the individual layer thickness, relaxed lattice parameters and bulk elastic constants of the materials that compose the MQW stack. Since the Eu content is small (~ 0.06), the elastic constants of the barrier and well can be considered the same. In this case, the in-plane lattice constant of the free-standing MQW structure is simply given by $a^{\text{fs}}=(d^{\text{barrier}}\times a^{\text{buffer}}+d^{\text{well}}\times a^{\text{PbTe}})/(d^{\text{barrier}}+d^{\text{well}})$, where $a^{\text{PbTe}}=6.462$ Å is the relaxed lattice constant of PbTe and a^{buffer} is the relaxed PbEuTe lattice constant, considered to be the same as for the buffer and barrier layers (same Eu content throughout each sample). The values of a^{fs} are displayed in Table I for all samples.

The reciprocal space map resolution does not allow an accurate determination of the in-plane lattice constant within the MQW structure, but it attests that the MQW tends to the free-standing condition. In order to obtain quantitatively the strain inside the MQWs, the (222) $\omega/2\theta$ spectrum of the MQW samples was calculated by dynamical theory of x-ray diffraction using Takagi–Taupin equations[14] and compared to the measured ones. The solid curves in Figs. 1 and 2 are the calculated spectra, which best fit to the measured data. The main fitting parameter is the in-plane lattice constant ($a^{\text{in-plane}}$) considered being the same throughout the whole MQW structure. Using this concept, the PbTe well has a tensile parallel strain given by $\epsilon_{||}^{\text{PbTe}}=(a^{\text{in-plane}}-a^{\text{PbTe}})/a^{\text{PbTe}}$, and the PbEuTe barrier remains with a compressive parallel strain $\epsilon_{||}^{\text{PbEuTe}}=(a^{\text{in-plane}}-a^{\text{buffer}})/a^{\text{buffer}}$. The perpendicular strain relates to the parallel strain through $\epsilon_{\perp}=-2[(c_{11}+2c_{12}-2c_{44})/(c_{11}+2c_{12}+4c_{44})]\epsilon_{||}$, where the c_{ij}'s are the elastic constants of the bulk material. In case of PbTe, $\epsilon_{\perp}=-1.09\epsilon_{||}$.

Figure 4 plots the $\omega/2\theta$ scan of sample M440 (PbTe well width of 104 Å), together with three calculated spectra using different values of $a^{\text{in-plane}}$. The best fit is obtained with $a^{\text{in-plane}}=6.4794$ Å and the other two curves are calculated using $a^{\text{in-plane}}=6.4820$ Å (PbTe well completely strained) and $a^{\text{in-plane}}=6.4768$ Å. This graph shows how sensitive the satellite peak position to the fitting parameter $a^{\text{in-plane}}$ is, i.e., the strain in the MQW structure.

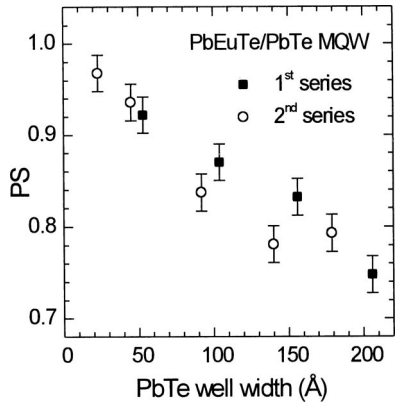

FIG. 5. Fraction of the maximum parallel strain incorporated in the PbTe well, $PS=\epsilon_{||}^{\mathrm{PbTe}}/\epsilon_{||}^{\mathrm{max}}$, as a function of the PbTe well width.

The maximum parallel strain for each MQW sample is given by $\epsilon_{||}^{\mathrm{max}}=(a^{\mathrm{buffer}}-a^{\mathrm{PbTe}})/a^{\mathrm{PbTe}}$, and a good parameter to describe the strain status in the MQW structure is the fraction of the maximum parallel strain incorporated in the PbTe well, $PS=\epsilon_{||}^{\mathrm{PbTe}}/\epsilon_{||}^{\mathrm{max}}$. The values of $a^{\text{in-plane}}$, $\epsilon_{||}^{\mathrm{PbTe}}$ and *PS* obtained from the best-fit procedure for all MQW samples are displayed in Table I. Figure 5 plots the parameter *PS* as a function of the PbTe well width. It decreases monotonically from 0.97 to 0.74 as the PbTe well width increases from 23 to 206 Å. This result means that the PbTe well is almost completely strained for samples with narrow wells and relaxes up to 26% of the maximum strain as the PbTe well width increases up to 200 Å. This graph represents the way the strain inside the PbTe well relieves as a function of its width for PbEuTe/PbTe MQW samples.

In a more realistic scenario, the in-plane lattice constant should vary within the MQW stack, i.e., a strain gradient probably exists through the MQW structure. It is important to point out that this gradient was not considered here and the value of $a^{\text{in-plane}}$ obtained from the fitting procedure gives the parallel strain averaged over the 50 periods that compose the MQW structure.

V. CONCLUSIONS

Two series of PbEuTe/PbTe MQW samples, in which the PbTe well width was varied from 23 to 206 Å, were successfully grown by molecular beam epitaxy. The Eu content in each series was 0.049 ± 0.003 and 0.059 ± 0.006. The well resolved satellite peak structure observed in the (222) $\omega/2\theta$ scans of all MQW samples indicated that very good thickness control and sharp interfaces were obtained. Reciprocal space mapping indicated that the MQW structure tended to the free-standing equilibrium condition. A broadening in ω direction was observed for all samples, indicating that some relaxation took place along the 50 periods of MQW structure. The calculated (222) $\omega/2\theta$ spectra were fitted to the experimental ones using the in-plane lattice constant as the main fitting parameter. The in-plane lattice constant obtained from the fitting procedure turned out to be slightly higher than the in-plane free-standing lattice parameter. The strain in the PbTe well inside the MQW structure decreased monotonically from an almost fully strained layer to 26% of strain relaxation as the PbTe well width increased from 23 to 206 Å. The actual strain obtained by this method has to be taken into account in the calculations of the energy structure of PbEuTe/PbTe MQW systems.

ACKNOWLEDGMENTS

The authors want to acknowledge Fundação de Amparo à Pesquisa do Estado de São Paulo - FAPESP (Project Nos. 95/6219-4, 97/06993-7 and 99/09049-3) and Conselho Nacional de Desenvolvimento Científico e Tecnológico - CNPq (Project Nos. 300397/94-1, 301091/95-1 and 300429/97-5) for financial support.

[1] 1 S. Yuan, H. Krenn, G. Springholz, A. Y. Ueta, G. Bauer, and P. J. McCann, Phys. Rev. B **55**, 4607 (1997).
[2] G. Springholz, G. Bauer, and G. Ihninger, J. Cryst. Growth **127**, 302 (1993).
[3] G. Springholz and G. Bauer, Appl. Phys. Lett. **60**, 1600 (1992).
[4] M. M. Olver, J. Z. Pastalan, S. E. Romaine, B. B. Goldberg, G. Springholz, G. Ihninger, and G. Bauer, Solid State Commun. **89**, 693 (1994).
[5] S. Yuan, G. Springholz, G. Bauer, and M. Kriechbaum, Phys. Rev. B **49**, 5476 (1994).
[6] S. Yuan, H. Krenn, G. Springholz, G. Bauer, and M. Kriechbaum, Appl. Phys. Lett. **62**, 885 (1993).
[7] E. A. de Andrada e Silva, Phys. Rev. B **60**, 8859 (1999).
[8] M. Kriechbaum, P. Kocevar, H. Pascher, and G. Bauer, IEEE J. Quantum Electron. **24**, 1727 (1988).
[9] D. L. Partin, IEEE J. Quantum Electron. **QE-24**, 1716 (1988), and references therein.
[10] G. Bauer, M. Kriechbaum, Z. Shi, and M. Tacke, J. Nonlinear Opt. Phys. Mater. **4**, 283 (1995).
[11] E. Koppensteiner, G. Springholz, P. Hamberger, and G. Bauer, J. Appl. Phys. **74**, 6062 (1993).
[12] S. O. Ferreira, E. Abramof, P. H. O. Rappl, A. Y. Ueta, H. Closs, C. Boschetti, P. Motisuke, and I. N. Bandeira, J. Appl. Phys. **84**, 3650 (1998).
[13] P. H. O. Rappl, H. Closs, S. O. Ferreira, E. Abramof, C. Boschetti, P. Motisuke, A. Y. Ueta, and I. N. Bandeira, J. Cryst. Growth **191**, 466 (1998).
[14] W. J. Bartels, J. Honstra, and D. J. W. Lobeek, Acta Crystallogr., Sect. A: Found. Crystallogr. **42**, 539 (1986).